Electron spin resonance and spin dynamics of two-dimensional diamagnetically diluted $Rb_2Mn_xCd_{1-x}Cl_4$ crystals

G. A. Petrakovskiĭ, L. S. Emel'yanova, I. T. Kokov, G. V. Bondarenko, and A. V. Baranov

Institute of Physics, Siberian Branch of the Academy of Sciences of the USSR, Akademgorodok

(Submitted 29 April 1982; resubmitted 12 August 1982)
Zh. Eksp. Teor. Fiz. **83**, 2176–2185 (December 1982)

The ESR method was used to study experimentally $Rb_2Mn_xCd_{1-x}Cl_4$ crystals with $x = 0.01$ and 0.4–1.0. At room temperature the ESR line width of these solid-solution crystals was governed by the slow diffusion component of the dipole–dipole interaction. Investigations of the ESR line profile, and of the angular dependences of the line width and resonance field intensity showed that a rapid change in the spin correlation function occurred in the case of compositions with $x < 0.62$. The magnetic percolation point for a two-dimensional square lattice was $x_c = 0.59$. The results demonstrated the effectiveness of the ESR method in investigating the characteristics of the spin correlation function at the magnetic percolation point.

PACS numbers: 76.30. − v, 75.25. + z

I. INTRODUCTION

When the concentration of magnetic ions is increased above the critical value $x > x_c$, a long-range magnetic order with $T_c > 0\,K$ is established and it is found that $T_c = 0\,°K$ for $x = x_c$. The critical concentration x_c is known as the magnetic percolation point and the magnetic properties of such systems are described using the percolation theory. Characteristics of this concentration-induced phase transition have been investigated experimentally by the neutron scattering method and have been modeled in numerical experiments.[1,2] In particular, it has been found that two-dimensional magnetic materils with a square lattice have the percolation threshold $x_c = 0.59$ (Ref. 3).

We investigated the phenomenon of magnetic percolation by the electron spin resonance (ESR) method. This method has been used successively to study crystal fields in the case of single-ion spectra ($x \approx 0.01$) and to determine the strength of the exchange interaction from the ESR spectra of ion pairs ($x = 0.03 - 0.1$).[4,5] Recent investigations of low-dimensional magnetic materials[6,7] have shown that the ESR method can give detailed information on the spin dynamics: the angular dependence of the ESR line width of low-dimensional magnetic materials is governed primarily by slow processes due to spin diffusion. Experimental investigations of $Rb_2Mn_xCd_{1-x}Cl_4$ (Ref. 3) and $K_2Mn_xMg_{1-x}Cl_4$ (Ref. 8) solid solutions have shown that the replacement of manganese ions with diamagnetic magnesium ions alters the angular and temperature dependences of the ESR line width. It can be shown that this is due to a change in the spin correlation function.

We shall give the results of a detailed investigation of the ESR line profile, as well as of the angualr dependences of the line width and resonance field of diamagnetically diluted $Rb_2Mn_xCd_{1-x}Cl_4$ crystals.

2. ELECTRON SPIN RESONANCE OF CONCENTRATED LOW-TEMPERATURE MAGNETIC MATERIALS

It is known[9] that the ESR line profile function represents the Fourier transform of the relaxation function $\Phi(t)$:

$$I(\Omega) = \frac{1}{2\pi}\int_{-\infty}^{\infty} \Phi(t)\, e^{i\Omega t} dt, \tag{1}$$

where $\Omega = \omega - \omega_0$ and ω_0 is the Larmor frequency. The relaxation function is of the form

$$\Phi(t) = \langle M^+(t) M^-(0)\rangle / \langle M^+ M^-\rangle, \tag{2}$$

where M is the trnsvese nonequilibrium magnetization. The relaxation function is related to the spin correlation function $\psi(\tau)$:

$$\Phi(t) = \exp\left[-\int_0^t (t-\tau)\,\psi(\tau)\, d\tau\right]. \tag{3}$$

The width of a Lorentzian ESR line is

$$\Delta H = \frac{2}{\gamma}\int_0^{\infty} \psi(\tau)\, d\tau. \tag{4}$$

Figure 1 shows schematically a spin correlation function of a low-dimensional system. The correlation function decreases rapidly in a time $\tau_1 \sim \hbar/J$, where J is the exchange integral in the plane of magnetic ions of two-dimensional magnetic materials or in a chain in the case of one-dimensional materials. In the case of three-dimensional magnetic materials the correlation function falls exponentially in the range $\tau > \tau_1$ obeying $\exp(-\Delta H_\tau)$ and the width of the ESR line is $\Delta H = M_2/\omega_{ex}$, where M_2 is the second moment of the line and ω_{ex} is the exchange frequency. In the case of low-dimensional magnet-

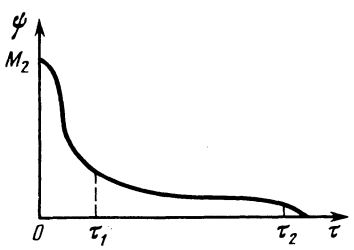

FIG. 1. Schematic representation of the spin correlation function $\psi(\tau)$ of Ref. 7: $\psi(\tau) \propto M_2 \exp(-\omega_{ex}{}^2\tau^2/2)$ in the range of short times, $0 < \tau < \tau_1$; $\psi(\tau) \propto \tau^{-d/2}$ in the diffusion region, $\tau_1 < \tau < \tau_2$.

 0038-5646/82/121260-06$04.00

ic materials the correlation function falls slowly in the range $\tau > \tau_1$ and in the approximation of a long time constant it can be described by $\psi(\tau) \propto \tau^{-d/2}$ (Ref. 6), where d is the dimensionality of the magnetic system. Diffusion decay of the correlation function continues up to $\tau_2 = \hbar/J_1$ (Ref. 7), where J_1 is the exchange integral of the interaction between magnetic layers in a two-dimensional lattice or the exchange integral of the interaction between magnetic chains in one-dimensional magnetic systems. An allowance for this diffusion contribution to $\psi(\tau)$ accounts for the non-Lorentzian line profile of one-dimensional magnetic materials and for the angular dependences of the ESR line width of low-dimensional magnetic systems. It is in the case of one-dimensional magnetic materials at temperatures $T \gg T_N$ that the main contribution to the line width is due to the spin diffusion processes with a wave vector $q = 0$ (Ref. 1a). The angular dependence of the line width is

$$\Delta H(\theta) = \alpha(3\cos^2\theta - 1)^{4/3} + \beta. \quad (5)$$

In the case of two-dimensional magnetic materials[6] we find that if $q = 0$, then

$$\Delta H(\theta) = \alpha(3\cos^2\theta - 1)^2 + \beta, \quad (6)$$

where θ is the angle between the chain axis and an external magnetic field in the case of one-dimensional systems or the angle between the noral to the layers and the external field in the case of two-dimensional materials; α and β are constants. The anisotropy of the ESR line width is not exhibited by three-dimensional cubic magnetic materials, whereas in the case of tetragonal crystals[11] we have

$$\Delta H(\theta) = \alpha(1 + \cos^2\theta) + \beta. \quad (7)$$

Here θ is the angle between the external field direction and the tetragonal axis of a crystal.

It thus follows that the angular dependences of the width and profile of an ESR line can be used to determine the nature of the correlation function.

3. SAMPLES AND EXPERIMENTAL METHOD

Single crystals of $Rb_2Mn_xCd_{1-x}Cl_4$ solid solutions ($x = 0.01, 0.4, 0.5, 0.62, 0.7, 0.8, 0.9$, and 1.0) were grown by the Bridgman melt method using the technology for the growth of ABX_3 chlorides.[12] The initial components $MnCl_2 \cdot 4H_2O$ and $CdCl_2 \cdot 2.5H_2O$ were heated in a chlorinating agent stream. Mixtures $RbCl + MnCl_2$ and $RbCl + CdCl_2$ were kept for days at temperatures 50 °C below the melting point. The synthesis and crystallization resulted from a slow displacement of a container with the melt from the maximum-heating zone to the cooling zone. Single crystals of Rb_2MnCl_4 and Rb_2CdCl_4 were obtained by the same method from $RbMnCl_3 + RbCl$ and $RbCdCl_3 + RbCl$. Solid solutions $Rb_2Mn_xCd_{1-x}Cl_4$ were prepared from melts with the stoichiometric ratios of Rb_2MnCl_4 and Rb_2CdCl_4. The solid-solution single crystals were transparent and they had a very pronounced cleavage plane perpendicular to the tetragonal axis. An investigation of the powder x-ray diffraction patterns of such solid solutions showed that all the samples were tetragonal with the D_{4h}^{17} symmetry.

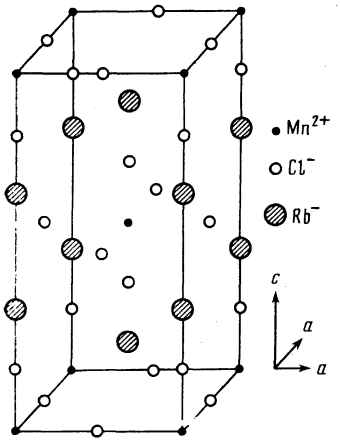

FIG. 2. Unit cell of Rb_2MnCl_4.

Figure 2 shows the structure of Rb_2MnCl_4. Ions of Mn^{2+} or Cd^{2+} are located at the centers of octahedra formed from Cl^- ions. Four octahedra bound by vertices form two-dimensional layers perpendicular to the c crystallographic axis. Layers of $[MnCl_6]^{4-}$ octahedra are separated by two layers of Rb ions. Single perovskite layers are shited relative to one another by half the diagonal of the unit cell. The magnetic structure Rb_2MnCl_4 is a set of antiferromagnetically ordered planes with a square network and these planes are separated by diamagnetic layers.[12]

The special nature of the magnetic structure is that for each Mn^{2+} ion there are equal numbers of parallel and antiparallel nearest neighbors in the adjacent planes, separated by $c/2$, which militates against ordering at right-angles to the layers. The interlayer exchange interaction with the ion under consideration is experienced only by the ions in the planes separated by the parameter c. The ratio of the interplanar exchange to the intraplanar interaction is $J_1/J = 10^{-6}$ (Ref. 12), so that we can regard Rb_2MnCl_4 as a two-dimensional magnetic material.

Figure 3 shows our measured unit cell parameters of the investigated solid solutions. Clearly, diamagnetic dilution increases linearly the distance between the magnetic ions in a layer, which is equal to the lattice cell parameter a, when the diamagnetic impurity concentration is increased. The dis-

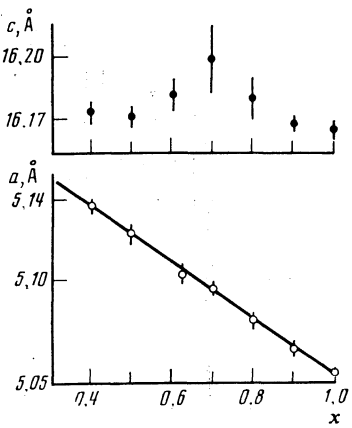

FIG. 3. Dependences of the unit cell parameters a and c on the magnetic ion concentration x in $Rb_2Mn_xCd_{1-x}Cl_4$.

tance between the layers changes only slightly. The concentration of the magnetic ions was found by the method of x-ray fluorescence analysis using a Spark-1 unit. The inhomogeneity of the distribution of Mn^{2+} ions in a crystal did not exceed 1%. The ESR spectra were investigated using an RÉ-1307 spectrometer ($\nu = 9.2$ GHz) at $T = 300$ °K.

4. EXPERIMENTAL RESULTS

a) Electron spin resonance spectra of Mn^{2+} ions in $Rb_2Mn_{0.01}Cd_{0.99}Cl_4$

Figure 4 shows the ESR spectrum of isolated Mn^{2+} ions in $Rb_2Mn_{0.01}Cd_{0.99}Cl_4$. An investigation of the angular dependences of the resonance fields showed that only one type of magnetic center is observed and Mn^{2+} ions replace Cd^{2+}. The distortion axis of the $[MnCl_6]^{4-}$ octahedron coincides with the c axis of the crystal. The angular dependences of the absorption lines can be described well by the spin Hamiltonian of axial symmetry[5]:

$$\hat{H}=g_{\parallel}\beta H_z\hat{S}_z+g_{\perp}\beta(H_x\hat{S}_x+H_y\hat{S}_y)+D[\hat{S}_z^2-{}^1/_3S(S+1)]+{}^1/_{180}F \times[35\hat{S}_z^4-30S(S+1)\hat{S}_z^2+25\hat{S}_z^2-6S(S+1)+3S^2(S+1)^2] +{}^1/_6a[\hat{S}_x^4+\hat{S}_y^4+\hat{S}_z^4-{}^1/_5S(S+1)(3S^2-3S-1)] +A\hat{S}_z\hat{I}_z+B(\hat{S}_x\hat{I}_x+\hat{S}_y\hat{I}_y), \quad (8)$$

where $g_{\parallel}$ and $g_{\perp}$ are the spectroscopic splitting factors; β is the Bohr magneton; **H** is an external magnetic field; $\hat{S}$ is the spin operator of an electron shell of Mn^{2+}; $S = 5/2$; D is a parameter of the axial crystal field; a and F are the parameters of the cubic crystal field; A and B are the parameters of the hyperfine interaction of the electron spin with the nuclear spin $I = 5/2$.

The absence of an anisotropy of the resonance fields in the *aa* plane (Fig. 2) shows that there is no orthorhombic distortion and that the cubic field parameters are small. A calculation of the resonance fields is made in the second order of perturbation theory using D, A, and B, and particularly a and F. This procedure gives the following parameters of the spin Hamiltonian (8):

$g_{\parallel}=1.998\pm0.0005$; $g_{\perp}=2.0000\pm0.0005$; $|D|=245\pm1$ Oe;
$A=-82.8\pm0.5$; $B=-86.4\pm0.5$ Oe;
$a=2\pm1$ Oe; $F=-4\pm1$ Oe

The g factors and the axial crystal field parameter were used later to calculate the anisotropy field in crystals with a high concentration of Mn^{2+} ions. In the case of $Rb_2Mn_xCd_{1-x}Cl_4$ ($x = 0.03$) there was a large number of weak lines in fields above and below the resonance fields of isolated Mn^{2+} ions. The ESR spectrum of weak lines was found to consist of groups of 11 components of the hyperfine structure. The distance between the absorption lines was 43 Oe, i.e., half the hyperfine interaction of isolated ions. These data indicated that the weak lines were due to the exchange-coupled pairs of Mn^{2+} ions. The angular dependences of these lines indicated that we are observing nearest pairs of Mn^{2+} ions located along the a axis.

b) Electron spin resonance in Rb_2MnCl_4

The compund Rb_2MnCl_4 exhibits a single absorption line of the Lorentzian profile. Static magnetic properties of Rb_2MnCl_4 were investigated in detail in Ref. 12. The spin Hamiltonian describing well the magnetic interactions is of the form

$$\hat{H}=-2J\sum_{ij}\hat{S}_i\hat{S}_j+g\beta\sum_i H\hat{S}_{z_i} +(g\beta)^2\sum_{i\neq j}\left[\frac{\hat{S}_i\hat{S}_j}{r_{ij}^3}-\frac{3(\hat{S}_i\mathbf{r}_{ij})(\hat{S}_j\mathbf{r}_{ij})}{r_{ij}^5}\right]+D\sum_i\hat{S}_{z_i}^2. \quad (9)$$

Here the first term is the Heisenberg exchange interaction (the summation is carried out over the nearest neighbors in the *aa* plane), whereas the second represents the Zeeman energy, and the third and fourth terms correspond to the dipole–interaction and to the single-ion anisotropy. The dominant contribution is that of the exchange interactions $2J = 7.7$ cm^{-1} (Ref. 12). The Zeeman energy for 9.2 GHz is 0.3 cm^{-1}. The energy of the dipole–dipole interaction was calculated by us using the formula

$$g^2\beta^2\sum_j r_{ij}^{-3}=0.2\text{ cm}^{-1}.$$

The single-ion anisotropy energy was estimated from the investigated single-ion ESR spectrum of Mn^{2+} in

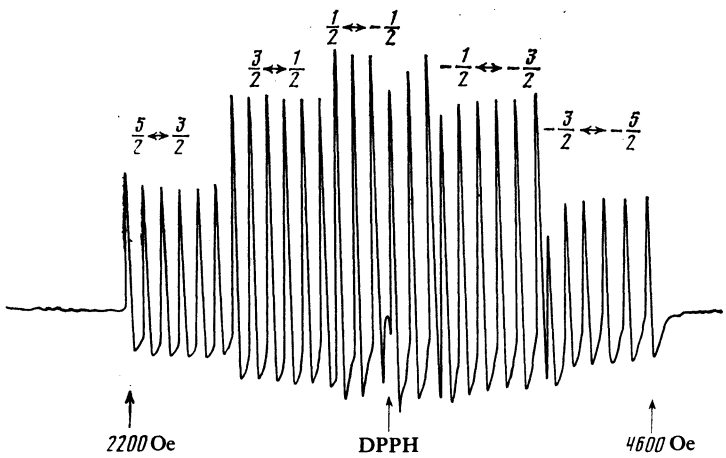

FIG. 4. Electron spin resonance spectrum of isolated Mn^{2+} ions in $Rb_2Mn_{0.01}Cd_{0.99}Cl_4$; $\mathbf{H}||c$.

$Rb_2Mn_{0.01}Cd_{0.99}Cl_4$: $D = 0.023$ cm^{-1}. Moreover, the anisotropy field in Rb_2MnCl_4 was found from the antiferromagnetic resonance data: $H_A = 1.7$ kOe (Ref. 13). The dipole contribution to the anisotropy field calculated by the Kornfel'd–Ewald method was found to be 1.39 kOe (Ref. 14). The single-ion anisotropy field was then 310 Oe = 0.029 cm^{-1}, in good agreement with the anisotropy parameter D calculated from the ESR spectrum.

It therefore follows that the single-ion anisotropy energy represents 10% of the energy of the dipole–dipole interaction. We shall ignore the single-ion anisotropy energy. Since the exchange interaction exceeds the Zeeman energy and the dipole–dipole interaction, we can use the calculations of the correlation function of two-dimensional systems carried out by Richards and Salamon.[6] The angular dependence of the line width, defined as the separation between the peaks of the absorption derivative, can be written in the following form in the case of two-dimensional magnetic materials[15]

$$\Delta H_{pp}(\theta) = (\pi/6)^{1/2}(M_2/\gamma\omega_{ex})(2+\sin^2\theta) + (K/3.46\gamma)$$
$$\times[\ln(\omega_{ex}/\omega_0) - 0.577](10\sin^2\theta\cos^2\theta + \sin^4\theta)$$
$$+ (K/3.46\gamma)\ln(\omega_{ex}/\omega_c)(3\cos^2\theta - 1)^2,$$
$$M_2 = 1.5S(S+1)\omega_d^2 W, \quad \omega_d = \frac{\hbar\gamma^2}{a^3}, \quad W = \sum_j \left(\frac{a}{r_{ij}}\right)^6,$$
$$K = \frac{3S(S+1)\omega_d^2 V^2}{32\pi D_d}, \quad V = \sum_j \left(\frac{a}{r_{ij}}\right)^3 = 9.05,$$
$$\omega_{ex} = \left(\frac{8S(S+1)z}{3}\right)^{1/2}\frac{J}{\hbar}, \qquad (10)$$

where $W = 4.65$ for a square lattice; $\gamma = 1.76\times10^7$ Oe^{-1} $\times$ sec^{-1}; z is the number of the nearest neighbors; ω_0 is the Larmor frequency; ω_c is the cutoff frequency of the diffusion tail of the correlation function. The diffusion parameter is $D_d = 0.3\omega_{ex}$ (Ref. 15). It is usually found at $\omega_c = \gamma\Delta H_{pp}$ (Ref. 7).

In the case of Rb_2MnCl_4 all the parameters are known and the line width can be represented as a function of the exchange integral J

$$\Delta H_{pp}[\text{Oe}] = \frac{12.6}{J}(2+\sin^2\theta) + \frac{5.89}{J}[\ln(21.4J) - 0.577]$$
$$\times(10\sin^2\theta\cos^2\theta + \sin^4\theta) + \frac{5.89}{J}(\ln 382J)(3\cos^2\theta - 1)^2, \qquad (11)$$

where J is in degrees Kelvin.

It therefore follows that in the case of two-dimensional Rb_2MnCl_4 all the three contributions to ΔH are important: the first represents the fast part of the dipole–dipole interaction; the second the slow diffusion part, i.e., its nondiagonal component; the third is the diagonal component of the diffusion contribution. It should be noted that in the case of three-dimensional magnetic materials the line width is governed by the first term in Eq. (10), whereas in the case of one-dimensional materials it is governed mainly by the third term in Eq. (10).

The angular dependences of the ESR line width of Rb_2MnCl_4 are plotted in Fig. 5. The experimental $\Delta H_{pp}(\theta)$ curve is described satisfactorily by the expression (11) with $J = 7.5 \pm 0.6$ °K. This value differs by 25% from J deduced from the static susceptibility χ measurements.[12] It is reported in Ref. 15 that J (ESR) and $J(\chi)$ differ by 30% in the case of two-dimensional antiferromagnets K_2MnF_4 and Rb_2MnF_4. This discrepancy can clearly decrease if we modify somewhat the calculation of the correlation function. Above all, an allowance should be made for the influence of the single-ion anisotropy on the ESR line width, as has been done in the case of one-dimensional magnetic materials.[16] First, it would be desirable to allow more rigorously for the exchange interactions (for example, for the exchange in the second coordination sphere and the interplanar exchange). Moreover, the diffusion parameters and the cutoff frequencies $\omega_c \sim 1/\tau_2$ will be defined further. These parameters can be deduced also from the neutron diffraction data.

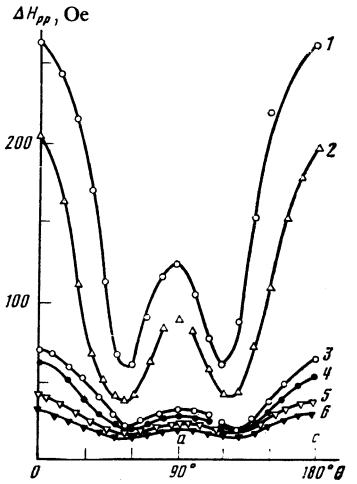

FIG. 5. Angular dependences of the ESR line width obtained for $Rb_2Mn_xCd_{1-x}Cl_4$ in the *ac* plane for different values of x: 1) 0.4; 2) 0.5; 3) 0.62; 4) 0.7; 5) 0.8; 6) 0.9 – 1.0.

c) Electron spin resonance of diamagnetically dilute $Rb_2Mn_xCd_{1-x}Cl_4$ ($1 > x \geqslant 0.4$) solid solutions

When the Mn^{2+} ion concentration was $x \geqslant 0.4$, it was found that the spectrum consisted of a single symmetric ESR line with $g = 2.004$. We investigated the profile of the derivative of the absorption line. We plotted in Fig. 6 the reciprocal amplitudes of the derivatives of the absorption line as a function of $[(H - H_0)/\Delta H_{pp}]^2$, where H_0 is the resonance field. A magnetic field was directed along the tetragonal axis of the crystal. The results (Fig., 6) indicated that in the case of compositions with $x < 0.62$ ($x = 0.5$ and 0.4) the line profiles differed strongly from Lorentzian and were the Fourier transforms of $\exp(-\gamma t)^{3/2}$. This expression was typical of one-dimensional systems. In the case of $\theta = 55°$ the line profile remained Lorentzian for all the compositions. These results indicated that diamagnetic dilution in the range $x < 0.62$ altered the slow rise of the correlation function from $\psi(\tau) \propto \tau^{-1}$ ($d = 2$) to $\psi(\tau) \propto \tau^{-1/2}$ ($d = 1$). A similar relationship applies also to $K_2Mn_xMg_{1-x}F_4$ (Ref. 8). The reason for the deviation of the ESR line profile for $x = 0.7$ and 0.8 is not yet clear.

The angular dependence of the line width $\Delta H_{pp}(\theta)$ in a

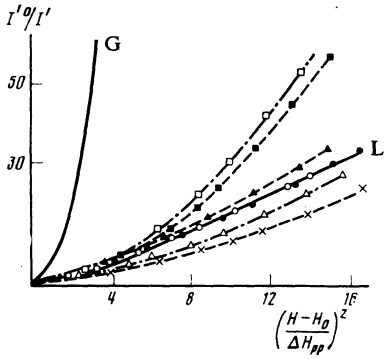

FIG. 6. Reciprocal amplitudes of the derivative of the ESR absorption line of $Rb_2Mn_xCd_{1-x}Cl_4$ for $\theta = 0°$ ($\mathbf{H}||c$) and different values of x: ○) 1.0; ●) 0.9; ×) 0.8; △) 0.7; ▲) 0.62; ■) 0.5; □) 0.4. The continuous curves show the Gaussian (G) and Lorentzian (L) line profiles. $I'^0 = I'(H - H_0 = \Delta H_{pp}/2)$.

plane perpendicular to the c axis is shown in Fig. 5. In the range $x < 0.62$ there was a steep increase in the anisotropy of the line profile. For all the compositions the minimum of the line profile was located at $\theta = 55 \pm 3°$, i.e., the greatest contribution to the line width was made by the third term in Eq. (10). The angualr dependence could be described satisfactorily by the formula

$$\Delta H_{pp}(\theta) = \alpha(3\cos^2\theta - 1)^2 + \beta. \qquad (12)$$

Table I gives the parameters α and β found by an analysis of the experimental data in Fig. 5 on a computer. In the case of the compositions with $x = 0.5$ and 0.4 the angular dependence $\Delta H_{pp}(\theta)$ was best described by the dependence $\alpha(3\cos^2\theta - 1)^{4/2} + \beta$ (the rms deviation of the calculated curve from the experimental results was twice as small in this case), which provided a further confirmation of changes in the time dependence of the correlation function in the range $x < 0.62$.

Figure 7 shows the concentration dependence of the line width ΔH_{pp} for $\theta = 0$ and 55°. In the $\theta = 0$ case the main contribution was due to diffusion processes which occurred

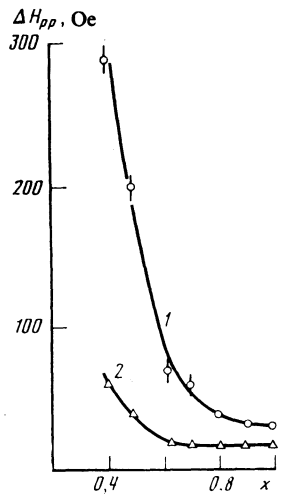

FIG. 7. Composition dependences of the ESR line width of $Rb_2Mn_xCd_{1-x}Cl_4$ for $\theta = 0°$ (1) and $\theta = 55°$ (2).

also in chains of finite length. Therefore, we could not expect a strong anomaly at the magnetic percolation flow. In the $\theta = 55°$ case the line width was governed by the slow dipole–dipole interaction processes and by diffusion processes averaged at the Larmor frequency. At the magnetic percolation point when infinite chains broke up, the exchange interactions could not affect significantly the ESR line narrowing. Therefore, below x_c we expected a strong increase in the line width, as found experimentally for $Rb_2Mn_xCd_{1-x}Cl_4$ at $\theta = 55°$, whereas in the $\theta = 0$ case we observed the monotonic rise of ΔH_{pp} even at low deviations of x from unity. This behavior of the ESR line width had been reported also for two-dimensional $Rb_2Mn_xMg_{1-x}F_4$ (Ref. 17) antiferromagnets, and in the latter case the line width was governed only by the fast part of the dipole–dipole interaction. The dependences of the resonance field on the angle θ for compositions with $x = 0.62 - 1.0$ were the same and were clearly due to the contribution of the average dipole field

$$H_{\text{dip}} = \langle \mu_z \rangle \sum_j (3\cos^2\theta_{ij} - 1) r_{ij}^{-3}, \qquad (13)$$

where r_{ij} is the distance between the magnetic ions and $\langle \mu \rangle_z$ is the average magnetic moment. In the case of solid solutions with $x = 0.5$ and 0.4 we found no resonance field anisotropy.

When the diamagnetic impurity concentration was increased, the anisotropy of the line width appeared and increased in the plane of a layer of Mn^{2+} ions. This dependence was of the form $(3\cos^2\theta - 1)^2$. Clearly, in the diamagnetic dilution case a network of magnetic ions became more mobile and the spin diffusion processes caused ΔH to change. The anisotropy of the line width in the aa plane was 5 Oe for $x = 0.8$; it was 12 Oe for $x = 0.5$ and 14 Oe for $x = 0.4$.

5. ESTIMATES OF THE EXCHANGE NARROWING PARAMETER OF ELECTRON SPIN RESONANCE LINES OF $Rb_2Mn_xCd_{1-x}Cl_4$

Exchange narrowing of an ESR line occurs when the exchange interaction is considerably stronger than the dipole–dipole interaction.[5] It is known that $(3\cos^2\theta - 1)^2$ in the range $\Delta H \propto M_2/\omega_{ex}$. In the case of concentrated atomically ordered magnetic crystals the exchange frequency ω_{ex} is proportionl to the exchange integral. In particular, in the case of two-dimensional magnetic materials,[15] we have

$$\omega_{ex} = [{}^8/_3 S(S+1)z]^{1/2} J/\hbar.$$

In view of the reduction in the number of exchange bonds per magnetic ion in the case of dilute magnetic materials, the exchange narrowing effect should become weaker. Such weakening can be described formally by introducing an exchange narrowing parameter of an ESR line $\tilde{J}(x)$. For convenience of comparison with the exchange parameter J of a Rb_2MnCl_4 crystal, we shall introduce the new quantity as follows:

$$\mathcal{J}(x) = \hbar\omega_{ex}[3/32S(S+1)]^{1/2}. \qquad (14)$$

Clearly, the parameter $\tilde{J}$ is a function of the distribution of the diamagnetic impurity over a crystal and of the exchange

TABLE I

x	1.0	0.9	0.8	0.7	0.62	0.5	0.4
α, Oe	3.95	3.5	5.7	9.5	11.5	39.5	52
β, Oe	12.8	13.9	16	18.1	23	39	74.5
R, Oe	0.6	0.9	0.5	1.0	4	9	17

Note. Here R is the average deviation of ΔH calculated using Eq. (12) from the experimental value.

integral of $Rb_2Mn_xCd_{1-x}Cl_4$. As pointed out earlier, the angular dependence $\Delta H_{pp}(\theta)$ for $\tilde{J}(x=1)=J=7.5\pm0.6$ °K yielded.... .

In the case of diamagnetically dilute two-dimensional systems there is no theory of a correlation function describing the change in the line width. Our ESR investigations of $Rb_2Mn_xCd_{1-x}Cl_4$ ($1\geqslant x\geqslant 0.62$) demonstrate that the nature of the dependences ΔH_{pp} and $H_0(\theta)$ is retained; therefore, in the calculation of the exchange narrowing parater $\tilde{J}(x)$ we shall use the correlation function approximation developed for two-dimensional magnetic materials.[6]

We shall rewrite the third term in the expression (10):

$$\alpha(x)=\frac{3S(S+1)\omega_d^2V^2}{3.46\gamma\cdot 32\pi\cdot 0.3\omega_{ex}}\ln\left(\frac{\omega_{ex}}{2\pi\gamma\Delta H_{pp}}\right)$$
$$=\frac{2\cdot 0.48\cdot 10^4x^2}{\tilde{J}(x)a^6(x)}\ln\left[\frac{7.2\cdot 10^4\tilde{J}(x)}{2\pi\Delta H_{pp}(x)}\right]. \qquad (15)$$

We shall take $\alpha(x)$ from Table I and the unit cell parameters from Fig. 3. We shall assume that the distribution of a diamagnetic impurity over a lattice is random, i.e., we shall postulate that[18]

$$\omega_d^2V^2=g^2\beta^2\left(\sum_j r_{ij}^{-3}\right)\sim x^2.$$

The exchange narrowing parameter of an ESR line calculated from Eq. (15) is given below:

x	1.0	0.9	0.8	0.7	0.62	0.5	0.4
$\tilde{J}$, °K	8±2	8±2	5.3±2	1.9±1	1.2±0.6	0.06±0.04	0.014±0.0

It should be noted that in the case of compositions with $x<0.62$ this parameter is close to zero.

6. CONCLUSIONS

It follows from our investigation that the ESR method can give detailed information on the magnetic interactions in $Rb_2Mn_xCd_{1-x}Cl_4$. Single-ion ESR spectra can give the g factor and the crystal field. These data can then be used to calculate the magnitude of the interactions governing the line width in the case of concentrated magnetic materials. The line width of Rb_2MnCl_4 is governed mainly by the dipole–dipole interaction and the greatest contribution is made by slow spin diffusion processes characterized by $q=0$.

In $Rb_2Mn_xCd_{1-x}Cl_4$, the concentration-dependent changes in the ESR line profile, the angular dependences of the line width in the *ac* and *aa* planes, the angular dependences of the resonance field H_0, and the calculated values of the exchange narrowing parameter of an ESR line all show that two-dimensional antiferromagnets belonging to the $Rb_2Mn_xCd_{1-x}Cl_4$ system exhibit considerable changes in the correlation function at compositions $x<0.62$. We can see that this is related to the magnetic percolation point. In the range $x<0.62$ the correlation function and particularly its slow part is close to the dependence $\psi(\tau)\sim\tau^{-1/2}$ typical of one-dimensional systems.

The authors are grateful to A. V. Borisov for his help with a computer analysis of the experimental data.

[1]S. Kirkpatrick, V sb.: Novosti fiziki tverdogo tela (Progress in Solid State Physics, Russ. Transl.), No. 7, Mir, M., 1977, p. 249.
[2]B. I. Shklovskiĭ and A. I. Éfros, Élektronnye svoĭstva legirovannykh poluprovodnikov (Electronic Properties of Doped Semiconductors), Nauka, M., 1979, Chap. 5.
[3]W. M. Walsh Jr, R. J. Birgeneau, R. W. Rupp Jr, and H. J. Guggenheim, Phys. Rev. B **20**, 4645 (1979).
[4]S. A. Al'tshuler and B. M. Kozyrev, Elektronnyĭ paramagnitnyĭ rezonans soedineniĭ élementov promezhutochnykh grupp (Electron Spin Resonance of Compounds of Intermediate-Group Elements), Nauka, M., 1972, Chap. 3.
[5]A. Abragam and B. Bleaney, Electron Paramagnetic Resonance of Transition Ions, Clarendon Press, Oxford, 1970 (Russ. Transl., t. 1, Mir, M., 1972, p. 484).
[6]P. M. Richards and M. B. Salamon, Phys. Rev. B **9**, 32 (1974).
[7]T. T. P. Cheung and Z. G. Soos, J. Chem. Phys. **69**, 3845 (1978).
[8]Y. Yokozawa, M. Tanimoto, and H. Takano, J. Phys. Soc. Jpn. **45**, 67 (1978).
[9]I. A. Aleksandrov, Teoriya magnitnoĭ relaksatsii (Theory of Magnetic Relaxation), Nauka, M., 1975, Chap. 3; Chap. 4, §12.
[10]R. E. Dietz, F. R. Merritt, R. Dingle, D. Hone, B. G. Silbernagel, and P. M. Richards, Phys. Rev. Lett. **26**, 1186 (1971).
[11]B. B. Garrett, C. F. Putnik, and S. L. Holt, Solid State Commun. **28**, 629 (1978).
[12]K. S. Aleksandrov (ed.), Fzovye perekhody v kristallakh galoidnykh soedineniĭ ABX_3 (Phase Transitions in ABX_3 Halide Crystals), Nauka, Novosibirsk, 1981, Chaps. 1,3.
[13]K. Strobel and R. Geick, Physica (Utrecht) B + C **108**, 951 (1981).
[14]N. V. Fedoseeva, I. P. Spevakova, A. N. Bazhan, and B. V. Beznosikov, Fiz. Tverd. Tela (Leningrad) **20**, 2776 (1978) [Sov. Phys. Solid State **20**, 1600 1978)].
[15]F. Ferrieu and M. Pomerantz, Solid State Commun. **39**, 707 (1981).
[16]A. Lagendijk, Physica (Utrecht) B + C **83**, 283 (1976).
[17]E. K. Henner and I. G. Shaposhnikov, Phys. Status Solidi A **55**, 315 (1979).
[18]B. I. Kochelaev, R. Kh. Sabirov, and G. G. Khaliullin, Fiz. Tverd. Tela (Leningrad) **19**, 152 (1977) [Sov. Phys. Solid State **19**, 86 (1977)].

Translated by A. Tybulewicz